Physical models for the design of photovoltaic/thermal collector systems

Y. Chaibi, T. El Rhafiki, R. Simón-Allué, I. Guedea, Cardamas Luaces, O. Charro Gajate, Tarik Kousksou, Y. Zeraouli

Physical models for the design of Photovoltaic/Thermal collector systems

Y. Chaibi[(a)], T. El Rhafiki[(a)], R. Simón-Allué[(b)], I. Guedea[(b)], Cardamas Luaces[(c)], O. Charro Gajate[(c)], T. Kousksou[(a)], Y. Zeraouli[(a)]

[(a)]Universite de Pau et des Pays de l'Adour, E2S UPPA, SIAME, Pau, France

[(b)]EndeF Engineering S.L., Pol. Ciudad del Transporte, 50820 Zaragoza, Spain

[(c)] KRD Global Group

Corresponding author.

E-mail address: chaibi.yassine@gmail.com,

Abstract

Solar photovoltaic thermal (PV/T) systems have the capacity to become a key actor in the world's energy transition. The design of such systems requires the implementation and development of physical models, which can predict their thermal and electrical performances. In this paper, some of the main models for designing PV/T systems are developed. In fact, various configurations of equivalent-circuit models are presented to perform the electrical behavior of PV/T systems. Further, a Quasi-Steady Thermal Model (QSTM) is developed to forecast thermal performances. All reported models are validated based on the literature results. The efficiency analysis of developed models demonstrates that the good choice of equivalent-circuit model is substantial and varies according to the climatic changes. Limitations of certain electrical models have also been outlined and discussed. This work could be a guideline to researchers for the physical modelling of PV/T systems.

***Keywords*:** PV/T collector systems; Thermal models; Equivalent-circuit models;

1. Introduction

In the context of the global debate on climate change, the building has become a strategic sector due to its high consumption of heat and electricity (Task 49 IEA, 2020; Task 60 IEA, 2020). About 50% of total energy consumption is used in the buildings in the European Union (EU) (European Commission, 2020; The European parliament, 2018). Solar energy, both thermal and photovoltaic, has considerable advantages to meet this challenge thanks to its growing competitiveness (Kousksou et al., 2015). In particular, PV/T hybrid solar system is promising with a double gain: the extraction of heat beneath the photovoltaic module generates both a gain in electrical efficiency and a gain through the use of this heat for the needs of the building (Jia et al., 2019; Lamnatou and Chemisana, 2017). PV/T systems can be easily integrated into the building without any major modification and they can be combined with other systems to supply heating and cooling depending on the season.

Most popular PV/T systems are designed with a cooling fluid flowing in an open loop (usually air) (Yang and Athienitis, 2014); or a closed-loop (usually water) (Yu et al., 2019), but there are also other PV/T collectors using a hybrid cooling system of air and water (Su et al., 2016). Water-based PV/T systems are more efficient than air-based PV/T systems due to their high thermo-physical properties (Chaibi et al., 2021a; Yu et al., 2019).

Over the last years, a significant number of research and development (R&D) works on PV/T technology have been carried out and various synthesis papers on PV/T systems have been published (Diwania et al., 2020; Kumar et al., 2015; Vaishak and Bhale, 2019). Several authors have been interested in PV/T air collectors due to their low manufacturing costs (Chaibi et al., 2021b; Ibrahim et al., 2011; Yazdanifard and Ameri, 2018).

The air cooling system provides a simple and economical solution for cooling the photovoltaic panels. Air can be heated to various temperature levels and its circulation can be either forced (via a fan) or natural. Forced circulation is required due to a better heat transfer by convection and conduction, however, the fan power consumption decreases the net electricity gain (Hussain et al., 2013).

A number of publications have been presented in recent years on the assessment of electrical, thermal and energy performance (Agrawal and Tiwari, 2013; Barone et al., 2019), or on the analysis of the profitability of these technologies by estimating the solar coverage rate (Abdul Hamid et al., 2014). Therefore, the development of thermal and electrical models has been

essential to examine the behaviour of these systems under steady-state or dynamic conditions (Yazdanifard and Ameri, 2018; Zondag, 2008).

Brinkworth (Brinkworth, 2002) simulated the convective and radiative phenomena occurring in the air gap in the air-based PV/T system. The author proposes a method to take into account the interaction between the two types of heat transfer and thus avoids the use of iterative methods generally used to estimate the radiative heat transfer. However, this model remains detailed and the knowledge of all its involved parameters is often lacking. Chow (Chow, 2003) published an explicit dynamic model to investigate the performances of the PV/T air collector.

Joshi and Tiwari (Joshi and Tiwari, 2007) presented an energy and exergetic analysis of an unglazed, Tedlar-coated air PVT hybrid solar collector. Their results indicated that the thermal and electrical efficiencies of the air PV/T collector are between 55-65% and 14-15% respectively.

Tonui and Tripanagnostopoulos (Tonui and Tripanagnostopoulos, 2007) developed a physical model of an air PV/T system using the analogy with the solar thermal collector model and experimental results. The model allows the calculation of the thermal and electrical efficiencies of the solar collector without requiring precise knowledge of its composition and without involving thermodynamic modelling. However, this model cannot be generalized. An experimental study is required to deduce the value of different coefficients to evaluate the thermal and electrical efficiency.

Sarhaddi et al. (Sarhaddi et al., 2010a, 2010b) performed an electrical and thermal model to evaluate the energetic and exergetic efficiency of a PV/T air collector. Some modifications concerning heat losses coefficients have been introduced to refine the thermal model of a PV/T air collector and a detailed single-diode equivalent-circuit model has been applied to ensure more accurate calculations of the electrical parameters of the PV/T air collector. A good agreement was found between the authors' numerical results and the experimental data. Shahsavar and Ameri (Shahsavar and Ameri, 2010) presented a physical model to evaluate the energy performance of a PV/T air collector, which is manufactured and tested under Kerman climate, Iran. A thin aluminium foil suspended in the middle of the air channel is inserted to improve the heat transfer surface and therefore the heat extraction from the PV panels. The PV/T air system is also tested in natural and forced convection. The authors'

results indicated that there was good agreement between the simulation and experimental data.

Elsafi and Gandhidasan (Elsafi and Gandhidasan, 2015) performed a physical model to investigate the effect of the fins design on the energy performance of a double-pass PV/T air collector. Three profiles of fins are tested and the impact of the number, thickness and the material of fins on the performance of the PV/T collector has also been discussed and presented by the authors. Simulation results demonstrated that pin fins are advantageous to achieve better performance compared to the straight fin design.

Bambrook and Sproul (Bambrook and Sproul, 2016) presented a RC circuit model to predict the energy performance of the PV/T air collectors under steady state conditions. According to the authors, this model can be used to rapidly and easily analyze the performance of PV/T air collectors that have a rather complex geometry.

This paper aims to present different physical models (thermal and electrical) that are currently used to describe the energy performance of a PVT air system. These models have been developed and experimentally validated under different conditions. These models have been compared to each other and some limitations in terms of accuracy have been outlined regarding the electrical models.

2. Thermal models

Fig.1 depicts the PV/T hybrid collector scheme considered in this work. It is constituted of a monocrystalline photovoltaic module with three layers: tempered glass, PV cells covered by two-ethylene vinyl acetate (*EVA*) layers and Tedlar (Sarhaddi et al., 2010a; Senthil Kumar et al., 2016).

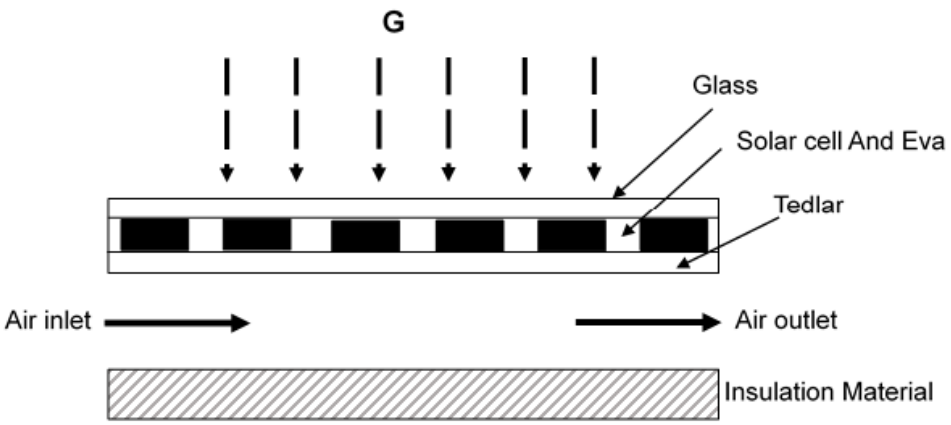

Fig.1: A cross-section picture of a PV/T air module.

2.1. Quasi-Steady Thermal Model (QSTM)

To describe a thermal model of the PV/T system under quasi-stationary conditions (Joshi and Tiwari, 2007), the following assumptions need to be made:

- By using the quasi-steady approximation, the temperature variation in each component layer is assumed as zero in each time step.
- The internal temperature variation along the thickness of each component layer is negligible.
- EVA has a transmissivity of approximately 100%;
- The airflow through the duct is uniform.
- The effect of temperature on the physical characteristics of each component layer is neglected.
- Heat loss is neglected as we consider the PV module to be well insulated.

Fig.2 presents the corresponding equivalent thermal resistance circuit and the size of the control volume for airflow.

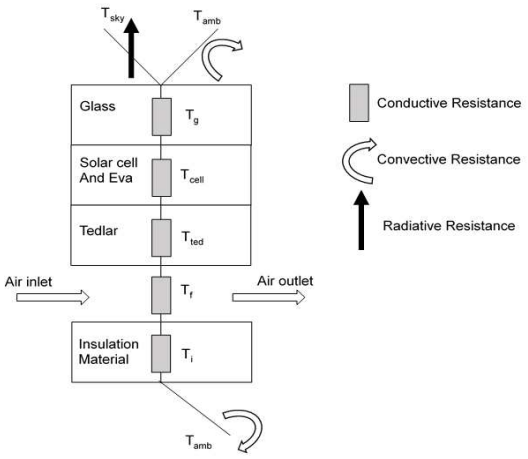

(a)

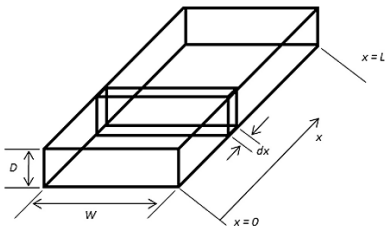

(b)

Fig.2: **(a)** Layout of thermal resistance system of a PV/T module, **(b)** basic length "dx" of a control volume (Sarhaddi et al., 2010a)

According to the law of conservation of energy, the energy balance equations for each component layer of the PV/T collector with air heating can be written as follows (Chow, 2003):

a) For glass

$$\alpha_g G = h_{rad}(T_g - T_{sky}) + h_c(T_g - T_{am}) + \frac{\lambda_g}{\delta_g}(T_g - T_c) \quad \textbf{(1)}$$

where, G is the solar radiation received by the glass, λ_g is the thermal conductivity of the glass, α_g is the absorptivity of the glass, T_{am} is the ambient temperature. Swinbank (Senthil Kumar et al., 2016) expression is used to estimate the sky temperature T_{sky}:

$$T_{sky} = 0.0552 T_{am}^{1.5} \quad \textbf{(2)}$$

McAdams correlation is adopted to determine the heat transfer coefficient between air and glass (Swinbank, 1963):

$$h_c = 5.7 + 3.8 V_{wind} \quad \textbf{(3)}$$

The radiative heat transfer coefficient term h_{rad} is calculated by using the following expression (Swinbank, 1963):

$$h_{rad} = \sigma \varepsilon_g (T_g^2 + T_{sky}^2)(T_g + T_{sky}) \quad \textbf{(4)}$$

where, σ and ε_g are Stefan Boltzmann constant and glass emissivity respectively.

b) For solar cell and Eva

$$G \beta_c \tau_g \alpha_{pv} - P_{pv} = \left[\frac{\delta_g}{\lambda_g} + \frac{\delta_c}{\lambda_c}\right]^{-1} (T_c - T_g) + \left[\frac{\delta_{ted}}{\lambda_{ted}} + \frac{\delta_c}{\lambda_c}\right]^{-1} (T_c - T_{ted}) \quad \textbf{(5)}$$

where, $\boldsymbol{\beta_c}$ is the packing factor, $\boldsymbol{\tau_g}$ is the glass transmittance, $\boldsymbol{\lambda_{ted}}$ is the thermal conductivity of the tedlar, $\boldsymbol{\lambda_c}$ is the thermal conductivity of the cell, $\boldsymbol{\delta_c}$ is the thickness of the cell, $\boldsymbol{\delta_{ted}}$ is the thickness of the tedlar and $\boldsymbol{\alpha_{pv}}$ is the absorptivity of the PV cells.

The electricity produced by PV cell (P_{pv}) can be calculated using the following expression (Sellami et al., 2019):

$$P_{pv} = G\beta_c\tau_g\eta_0\left[1-\beta\left(T_c - T_{ref}\right)\right] \quad \textbf{(6)}$$

where, $\boldsymbol{\beta}$ is the cell temperature coefficient and $\boldsymbol{\eta_0}$ is the reference electrical efficiency of PV panel for a reference temperature T_{ref}.

c) For Tedlar

$$h_f\left(T_{ted} - T_f\right) = \left[\frac{\delta_{ted}}{\lambda_{ted}} + \frac{\delta_c}{\lambda_c}\right]^{-1}\left(T_c - T_{ted}\right) \quad \textbf{(7)}$$

where, $\boldsymbol{h_f}$ is the heat transfer coefficient between air and the tedlar.

d) For air

$$c_f\dot{m}_f\frac{\partial T_f}{\partial x} = h_f W\left(T_{ted} - T_f\right) \quad \textbf{(8)}$$

where, $\boldsymbol{\dot{m}_f}$ is the mass flow rate of air and W is the PV/T width.

From **Eqs.(1)**, **(5)**, **(7)** and **(8)**, the air temperature $T_f\ (x,t)$ can be obtained by integrating **Eq. (8)** with the initial condition $T_{f,in} = T_f\big|_{x=0}$ as:

$$T_f(x) = \frac{Y_1}{Y_2}\left(e^{Y_2 x} - 1\right) + T_f(x=0)e^{Y_2 x} \quad \textbf{(9)}$$

where, Y_1 and Y_2 are functions depending on the thermophysical properties of the PV/T system, the thickness of each layer (glass, solar cell+Eva and Tedlar), the airflow rate, the ambient temperature T_{am} and the solar radiation G.

The outlet temperature of air can be determined from the above equation as:

$$T_f(x=L) = \frac{Y_1}{Y_2}\left(e^{Y_2 L} - 1\right) + T_f(x=0)e^{Y_2 L} \quad \textbf{(10)}$$

where, L is the length of the collector. Y_1 and Y_2 are given by the following expressions:

$$Y_2 = \frac{h_f W}{\dot{m}c_f}\left(\frac{h_f}{h_f + c_1} + \frac{c_1}{h_f + c_1}\frac{d_3}{d_2} - 1\right)$$

(10.1)

$$Y_1 = \frac{h_f W}{\dot{m}c_f}\frac{c_1}{h_f + c_1}\frac{d_1}{d_2}$$

(10.2)

where:

$$\boldsymbol{d_1 = b_1 + b_2\frac{a_1}{a_2}}$$

(10.3)

$$\boldsymbol{d_2 = b_2 + b_3 - \frac{b_3 c_1}{h_f + c_1} + b_2 \frac{a_3}{a_2}}$$

(10.4)

$$\boldsymbol{d_3 = \frac{b_3 h_f}{h_f + c_1}}$$

(10.5)

$$\boldsymbol{a_1 = \alpha_g G + h_{rad} T_{sky} + h_c T_{am}}$$

(10.6)

$$a_2 = h_{rad} + h_c + \frac{\lambda_g}{\delta_g}$$

(10.7)

$$a_3 = \frac{\lambda_g}{\delta_g}$$

(10.8)

$$b_1 = G \beta_c \tau_g \alpha_{pv} - P_{pv}$$

(10.9)

$$\boldsymbol{b_2 = (\frac{\lambda_g}{\delta_g} + \frac{\lambda_c}{\delta_c})^{-1}}$$

(10.10)

$$b_3 = (\frac{\lambda_{ted}}{\delta_{ted}} + \frac{\lambda_c}{\delta_c})^{-1}$$

(10.11)

2.2. Transient Thermal Model (TTM)

To perform the energy balance for each layer of the PV/T module, various assumptions have been applied:

- Unsteady model means that: $\frac{\partial T_i}{\partial t} \neq 0$, where *i* = glass, PV cell and air;
- EVA has a transmissivity of approximately 100%;
- the airflow through the duct is uniform;
- the effect of temperature on the physical characteristics of each component layer is neglected;
- the temperature of glass, cell, tedlar and air depends only on the longitudinal dimension in the flow direction;
- the heat transfer by conduction along the flow direction in each layer is considered.

- heat loss is neglected as we consider the PV module to be well insulated.

The thermal energy equations for various layers of the system are as follows:

a) Energy equation for glass

$$(\rho c\delta)_g \frac{\partial T_g}{\partial t} = \lambda_g \delta_g \frac{\partial^2 T_g}{\partial x^2} + \alpha_g G + \sigma \varepsilon_g \left(T_{sky}^4 - T_g^4\right) + h_c \left(T_{am} - T_g\right) + \frac{\lambda_g}{\delta_g}\left(T_c - T_g\right)$$

(11)

where, ρ_g is the density of the glass, c_g is the heat capacity of the glass and λ_g is the thermal conductivity of the glass.

b) Energy equation for PV cell

$$(\rho c\delta)_c \frac{\partial T_c}{\partial t} = \lambda_c \delta_c \frac{\partial^2 T_c}{\partial x^2} + \left[\frac{\delta_g}{\lambda_g} + \frac{\delta_c}{\lambda_c}\right]^{-1} \left(T_g - T_c\right) + \left[\frac{\delta_{ted}}{\lambda_{ted}} + \frac{\delta_c}{\lambda_c}\right]^{-1} \left(T_{ted} - T_c\right) + G\beta_c \tau_g \alpha_{pv} - P_{pv}$$

(12)

where, ρ_c is the density of the solar cell, c_c is the heat capacity of the cell and λ_c is the thermal conductivity of the cell.

c) Energy equation for Tedlar

$$(\rho c\delta)_{ted} \frac{\partial T_{ted}}{\partial t} = \lambda_{ted} \delta_{ted} \frac{\partial^2 T_{ted}}{\partial x^2} + h_f \left(T_f - T_{ted}\right) + \left[\frac{\delta_{ted}}{\lambda_{ted}} + \frac{\delta_c}{\lambda_c}\right]^{-1} \left(T_c - T_{ted}\right) \quad \textbf{(13)}$$

where, ρ_{ted} is the density of the tedlar, c_{ted} is the heat capacity of the tedlar and λ_{ted} is the thermal conductivity of the tedlar.

d) Energy equation for air

$$(\rho cA)_f \frac{\partial T_f}{\partial t} + c_f \dot{m}_f \frac{\partial T_f}{\partial x} = \lambda_f A_f \frac{\partial^2 T_f}{\partial x^2} + h_f W \left(T_{ted} - T_f\right) \quad \textbf{(14)}$$

where, ρ_f is the density of the air, c_f is the heat capacity of the air and λ_f is the thermal conductivity of the air, $\dot{m}_f$ is the mass flow rate of air and A_f is the cross-sectional area of the fluid and W is the PV/T width.

A fully implicit finite volume method was used to solve the energy equations system. The first-order upwind scheme was applied to address convective terms, and diffusion terms are discretized using the second order of the central differential scheme**.** Therefore, the resulting expression of the system of energy equations is as follows:

e) Energy equation for glass

$$A_{i,g}T_{i,g}^{t+\Delta t} = A_{i+1,g}T_{i+1,g}^{t+\Delta t} + A_{i-1,g}T_{i-1,g}^{t+\Delta t} + C_{i,g} \quad \textbf{(15)}$$

Where:

$$A_{i,g} = \frac{(\rho c\delta)_g}{\Delta t} + \frac{2\lambda_g\delta_g}{\Delta x^2} + h_r + h_c + \frac{\lambda_g}{\delta_g} \quad \textbf{(16)}$$

$$A_{i+1,g} = \frac{\lambda_g\delta_g}{\Delta x^2} \quad \textbf{(17)}$$

$$A_{i-1,g} = \frac{\lambda_g\delta_g}{\Delta x^2}$$

(18)

$$\boldsymbol{C_{i,g} = \frac{(\rho c\delta)_g}{\Delta t}T_{i,g}^{t} + h_c T_{am}^{t+\Delta t} + h_r T_{sky} + \frac{\lambda_g}{\delta_g}T_{i,c}^{t+\Delta t} + \alpha_g G^{t+\Delta t}} \quad \textbf{(19)}$$

$$h_r = \sigma\varepsilon_g\left(T_{sky}^2 - T_g^{2,t}\right)\left(T_{sky} - T_g^t\right)$$

(20)

f) Energy equation for PV cell

$$A_{i,c}T_{i,c}^{t+\Delta t} = A_{i+1,c}T_{i+1,c}^{t+\Delta t} + A_{i-1,c}T_{i-1,c}^{t+\Delta t} + C_{i,c}$$

(21)

Where:

$$A_{i,c} = \frac{(\rho c\delta)_c}{\Delta t} + \frac{2\lambda_c\delta_c}{\Delta x^2} + B_1 + B_2 - \tau_g\beta_c G^{t+\Delta t}\eta_0\beta$$

(22)

$$A_{i+1,c} = \frac{\lambda_c\delta_c}{\Delta x^2}$$

(23)

$$A_{i-1,c} = \frac{\lambda_c\delta_c}{\Delta x^2}$$

(24)

$$C_{i,c} = \frac{(\rho c\delta)_c}{\Delta t}T_{i,c}^{t} + B_1 T_{i,g}^{t+\Delta t} + B_2 T_{i,ted}^{t+\Delta t} + \tau_g\beta_c G^{t+\Delta t}\left(\alpha_{pv} - \eta_0\right) - \tau_g\beta_c G^{t+\Delta t}\eta_0\beta T_{ref}$$

(25)

where, $B_1 = \left[\frac{\delta_g}{\lambda_g} + \frac{\delta_c}{\lambda_c}\right]^{-1}$ and $B_2 = \left[\frac{\delta_{ted}}{\lambda_{ted}} + \frac{\delta_c}{\lambda_c}\right]^{-1}$

g) Energy equation for Tedlar

$$A_{i,ted}T_{i,ted}^{t+\Delta t} = A_{i+1,ted}T_{i+1,ted}^{t+\Delta t} + A_{i-1,ted}T_{i-1,ted}^{t+\Delta t} + C_{i,ted} \quad \textbf{(26)}$$

Where:

$$A_{i,ted} = \frac{(\rho c\delta)_{ted}}{\Delta t} + \frac{2\lambda_{ted}\delta_{ted}}{\Delta x^2} + B_2 + h_f \quad \textbf{(27)}$$

$$A_{i+1,ted} = \frac{\lambda_{ted}\delta_{ted}}{\Delta x^2} \quad \textbf{(28)}$$

$$A_{i-1,ted} = \frac{\lambda_{ted}\delta_{ted}}{\Delta x^2} \quad \textbf{(29)}$$

$$C_{i,ted} = \frac{(\rho c\delta)_{ted}}{\Delta t} T_{i,ted}^{t} + B_2 T_{i,c}^{t+\Delta t} + h_f T_{i,f}^{t+\Delta t} \quad \textbf{(30)}$$

h) Energy equation for air

$$A_{i,f} T_{i,f}^{t+\Delta t} = A_{i+1,f} T_{i+1,f}^{t+\Delta t} + A_{i-1,f} T_{i-1,f}^{t+\Delta t} + C_{i,f} \quad \textbf{(31)}$$

Where:

$$A_{i,f} = \frac{(\rho c\delta)_f}{\Delta t} + \frac{2\lambda_f \delta_f}{\Delta x^2} + h_f W \quad \textbf{(32)}$$

$$A_{i+1,f} = \frac{\lambda_f \delta_f}{\Delta x^2} - \frac{c_f \dot{m}_f}{2\Delta x} \quad \textbf{(33)}$$

$$A_{i-1,f} = \frac{\lambda_f \delta_f}{\Delta x^2} + \frac{c_f \dot{m}_f}{2\Delta x} \quad \textbf{(34)}$$

$$C_{i,f} = \frac{(\rho cA)_f}{\Delta t} T_{i,f}^{t} + W h_f T_{i,ted}^{t+\Delta t} \quad \textbf{(35)}$$

The system of equations **(11, 17, 22** and **27)** needs to be closed by considering the following boundary conditions:

$$\frac{\partial T_g(x,t)}{\partial x} = \frac{\partial T_c(x,t)}{\partial x} = \frac{\partial T_{ted}(x,t)}{\partial x} = 0 \text{ at } x = 0 \text{ and } x = L \quad \textbf{(36)}$$

$$\frac{\partial T_f(x,t)}{\partial x} = 0 \quad \text{at} \quad x = L \quad \textbf{(37)}$$

$$T_f(x,t) = T_{am}(t) \quad \text{at} \quad x = 0 \quad \textbf{(38)}$$

Equation 36 signifies that the extremities of the three layers of the collector are assumed to be perfectly insulated. We supposed that the air flow reaches its steady state at the outlet of the collector (**Eq.37**) and the air temperature at the inlet of the collector is equal to the ambient temperature (**Eq.38**).

In this paper, **Eqs. 15**, **21**, **26** and **31** were solved iteratively by using a Tridiagonal Matrix Algorithm (TDMA) method (Joshi et al., 2009). The computation procedure was carried out using Fortan 90. The specified iteration in each time interval was considered convergent

when the maximum relative residual of T_g, T_c, T_{ted} *and* T_f was less than 10^{-4}. The general procedure for the numerical simulation can be outlined in the following steps (see **Fig.3**):

1. Set the physical properties of PV/T module.
2. Introduce inlet air temperature, inlet air mass flow rate and solar irradiance.
3. Calculate all coefficients of **Eqs. 15**, **21**, **26** and **31**.
4. Solve **Eqs**. **15**, **21**, **26** and **31** with TDMA algorithm.
5. Control the test convergence and terminate the iterative process, if necessary.
6. Otherwise, use new values and go to 2.
7. Save the obtained values and stop.

2.3. Thermal and electrical efficiencies of the PV/T system

The thermal (η_{th}) and electrical efficiency (η_{ele}) are calculated as (Evans, 1981; Hosseinzadeh et al., 2018):

$$\eta_{th} = \frac{c_f \dot{m}_f (\bar{T}_f - T_{f,in})}{G A_{pv}} \quad \textbf{(39)}$$

$$\eta_{ele} = \eta_{ref} \beta_c [1 - 0.0045(\bar{T}_c - 298.15)] \quad \textbf{(40)}$$

where, $\bar{T}_c$ is the average temperature of the PV cell and $\bar{T}_f$ is the average temperature of the fluid (Hazami et al., 2016). In this work the reference efficiency η_{ref} is assumed to be 12%, which is in the range of the efficiency of common PV modules (Good, 2016).

The overall energy efficiency of the PV/T module is calculated using the following expression (Patankar, 1980):

$$\eta_g = \eta_{th} + \frac{\eta_{ele}}{C_F} \quad \textbf{(41)}$$

The electrical energy conversion factor C_F ranges from 0.35 to 0.40 and is generally used for PVT systems (Joshi et al., 2009).

The numerical solution procedure is explained in **Fig.3**.

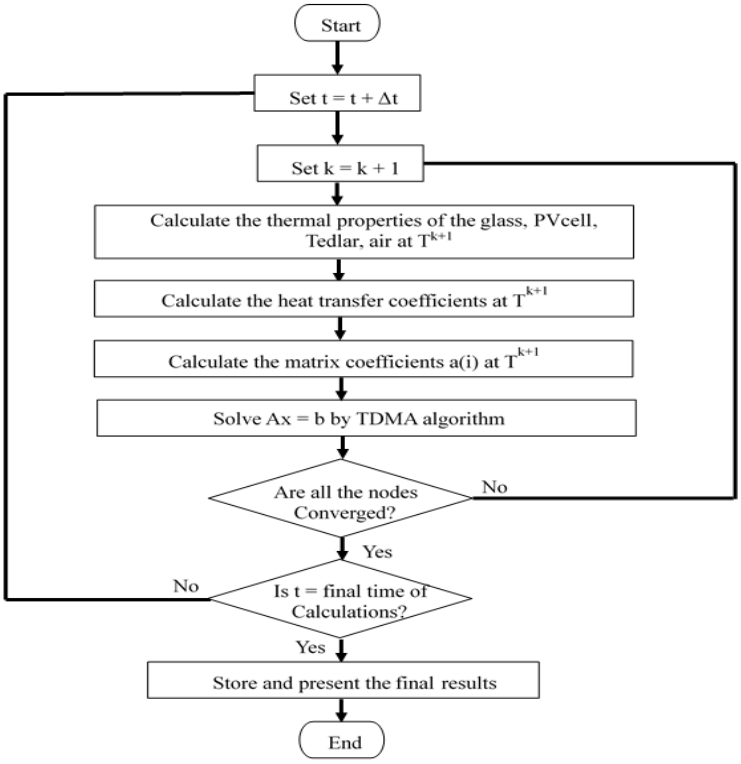

Fig.3: Flowchart of the numerical process

2.4. Experimental validation

Numerical results obtained by the present model are compared to the experimental results reported by Joshi et al. (Joshi et al., 2009). The experimental apparatus of Joshi et al. (Joshi et al., 2009) include two monocrystalline silicon PV modules integrated with an air duct. The electrical energy generated with PV modules is stored in a battery. Two DC fans blow air into air duct. The DC fans consume a small amount of electricity from the battery itself, which is neglected during the simulation. The measurements have been recorded during a clear day from 8:00 a.m to 5:00 p.m on May at Solar Energy Park, IIT Delhi (India). The experimental data have been recorded every hour. Solar radiation intensity, ambient temperature, air temperature at the inlet and outlet of the PV/T, and PV cell temperature are some of the parameters that Joshi et al. (Joshi et al., 2009) have measured. The design parameters and thermophysical properties of the PV/T air collector are presented in **Table 1** (Sarhaddi et al., 2010a). **Fig. 4** indicates the experimental day's variations in solar radiation intensity, ambient temperature and inlet air temperature. **Fig.5** illustrates the variation versus time of the air temperature at the output of the PVT module, the average PV cell temperature and the related experimental data. Based on this figure, there is generally a good correspondence between experimental and numerical results. The thermal and electrical efficiencies of the PV/T air

system are illustrated in **Fig.6.** From figure, it can be seen that there is a reasonable agreement between experimental and calculated values of these efficiencies. The difference between the experimental and calculated efficiencies can be explained as follows:

- Wind speed is considered constant. However, in practice this velocity is not constant and has a direct effect on the heat loss through the system;
- The absorption and transmission coefficients were considered constant while they vary over the day as solar incidence angle on the PV/T system surface changes.

Table 1: Design parameters of the PV/T air module (Senthil Kumar et al., 2016)

Solar PVT air module parameters	**Value**
PV module type	Siemens SP75, monocrystalline silicon
The number of cells in series, N_c	36
The maximum power of PV module at STC, $P_{pv,MPP}$	75 W
The maximum voltage of PV module at STC, $V_{pv,MPP}$	17 V
The maximum current of PV module at STC, $I_{pv,MPP}$	4.4 A
The short-circuit current of PV module at STC, I_{sc}	4.8 A
The open-circuit voltage of PV module at STC,V_{oc}	21.7 V
The temperature coefficient of I_{sc}, K_i	2.06 mA/°C
The length of PV module, L	1.2 m
The width of PV module, W	0.527 m
The area of PV module, S_m	0.632 m^2
The electrical efficiency at the reference conditions, $\eta_{ele,ref}$	0.12
The density of glass cover, ρ_g	2450 $kg.m^{-3}$
The specific heat capacity of glass cover, c_g	500 $J.kg^{-1}.K^{-1}$
The thickness of glass cover, δ_g	0.003 m
The conductivity of glass cover, λ_g	1 $W.m^{-1}.K^{-1}$
The transmissivity of glass cover, τ_g	0.95
The conductivity of solar cell, λ_c	130 $W.m^{-1}.K^{-1}$
The specific heat capacity of solar cell, c_c	677 $J.kg^{-1}.K^{-1}$
The density of solar cell, ρ_c	2330 $kg.m^{-3}$
The absorptivity of solar cell, α_c	0.85
The thickness of solar cell, δ_c	0.0003 m
The conductivity of solar cell, λ_c	0.036 $W.\ m^{-1}.K^{-1}$
The thickness of tedlar, δ_{ted}	0.0005 m
The conductivity of tedlar, λ_{ted}	0.033 $W.\ m^{-1}.K^{-1}$
The specific heat capacity of tedlar, c_{ted}	1250 $J.kg^{-1}.K^{-1}$
The density of tedlar, ρ_{ted}	1200 $kg.m^{-3}$
The duct depth, δ_{air}	0.05 m
The conversion factor C_f	0.36
The packing factor β_c	0.83
Inlet air velocity, V_i	0.1 $m.s^{-1}$

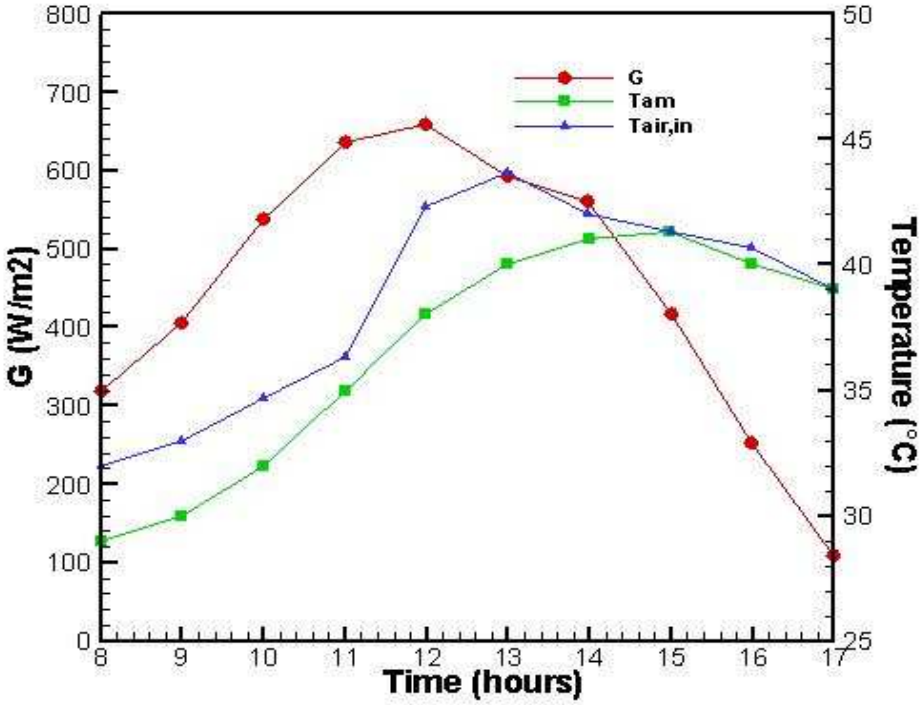

Fig.4: The hourly variation of G, T_{am} and $T_{air,inlet}$

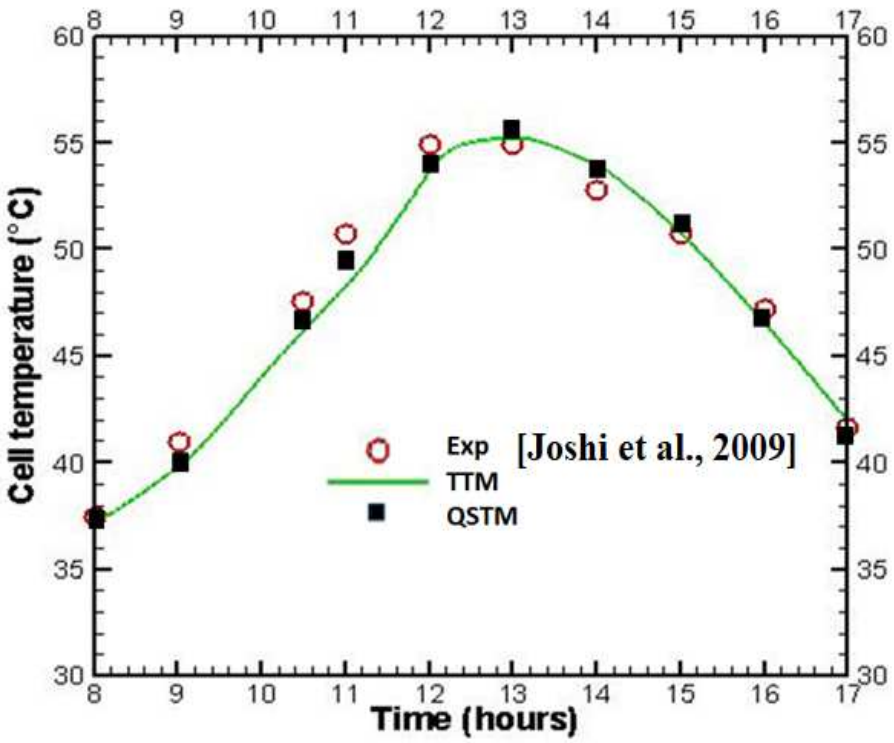

(a)

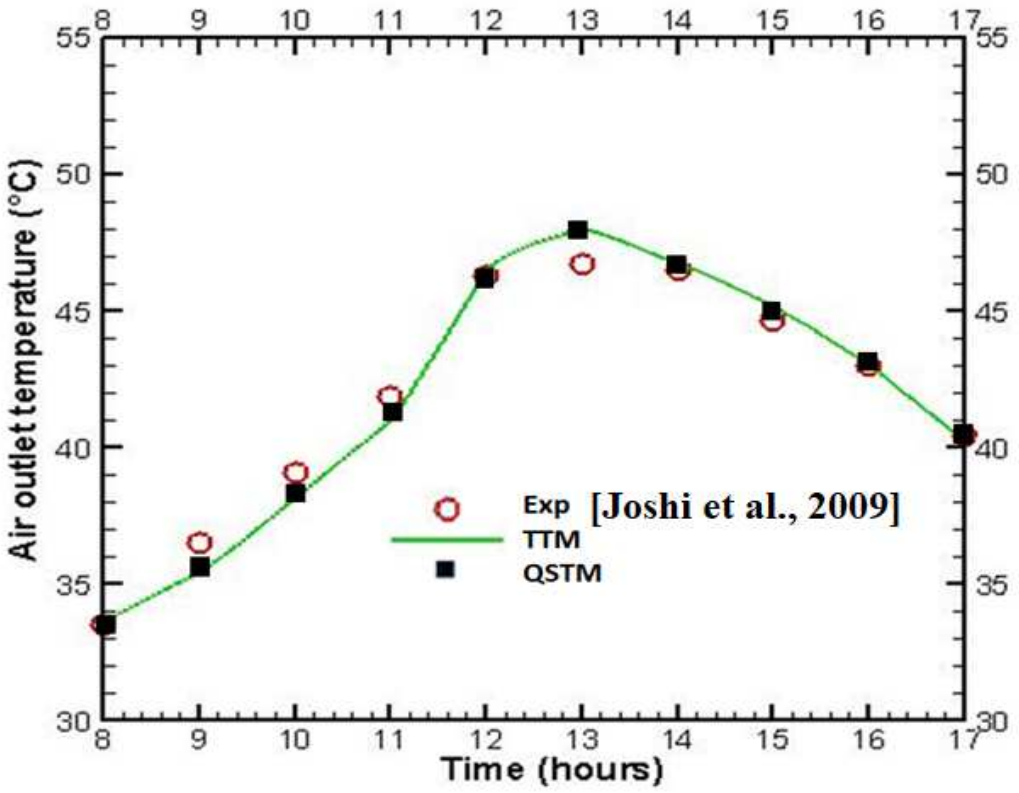

(b)

Fig.5: Numerical and experimental results: **(a)** Outlet air temperature, **(b)** Average cell temperature

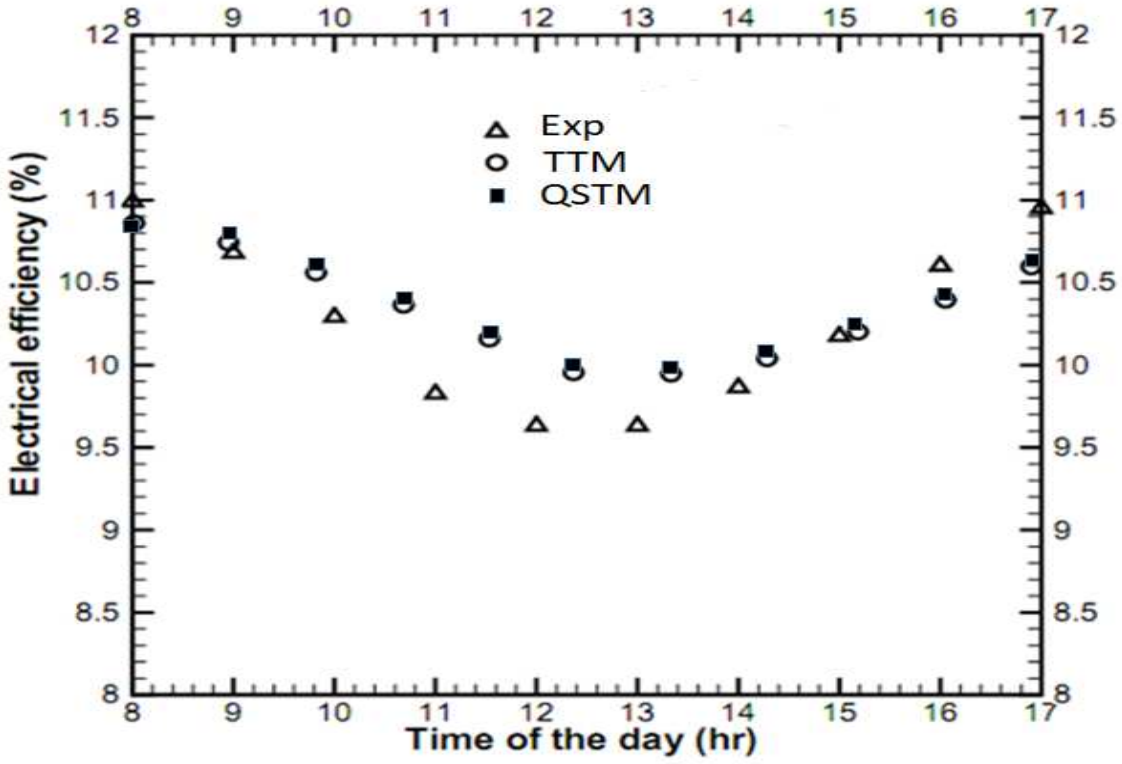

(a)

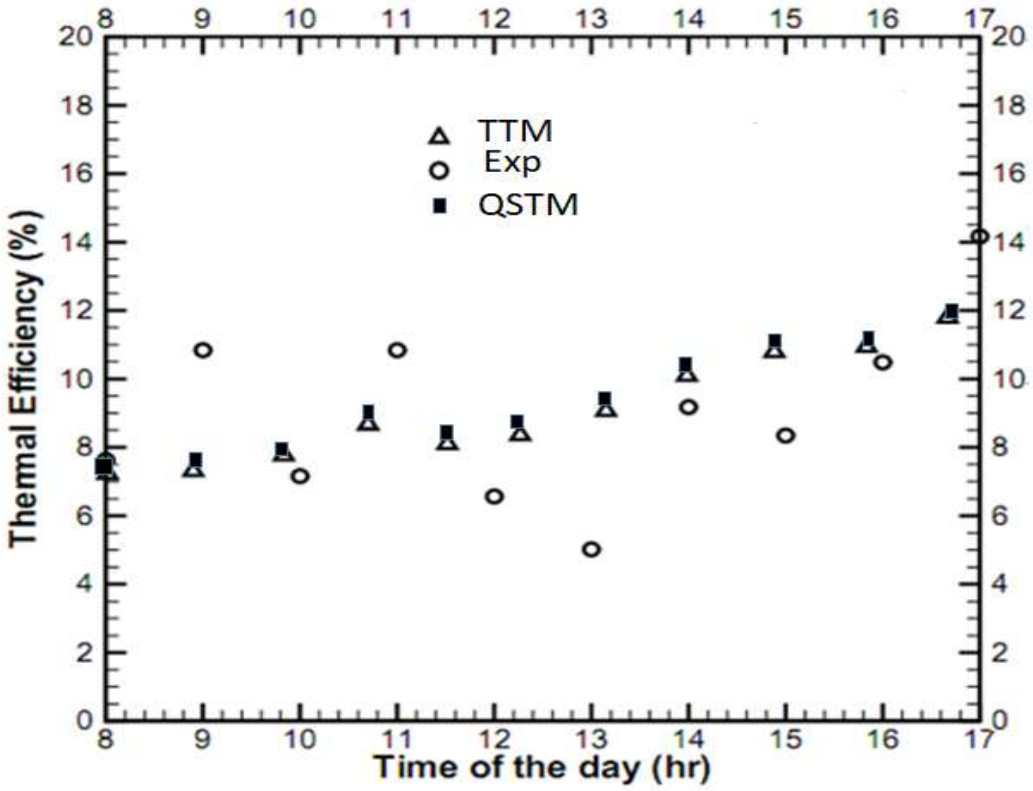

(b)

Fig.6: Efficiencies of the PV/T versus time: **(a)** Electrical efficiency and **(b)** Thermal efficiency

It is interesting to note that for the quasi-stationary model (QSTM), the heat transfer by conduction according to the direction of airflow has been neglected within each layer of the system. To study the importance of this phenomenon on the performance of PV/T, we compared the evolution of the temperature provided by the two models (QSTM and TTM) at each layer level as a function of *x* (see **Fig.7**).

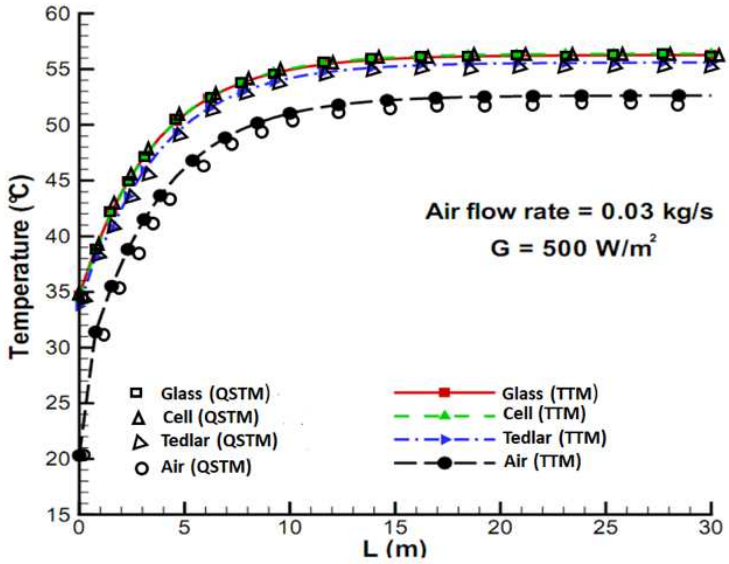

Fig.7: Outlet air temperature for different lengths of the collector.

An examination of the simulated curves under the same conditions shows a very small influence of this heat transfer phenomenon by conduction on the evolution of temperatures at the level of each layer. The absence of heat diffusion by conduction following the direction of flow in each layer of the system has no significant impact on the performance of the system. We can also note that the heat transfer between the cells and the air is highest at the inlet of the PV/T air collector at which there is the highest temperature difference between the fluid and the PV cells. Towards the output of the long PV/T air collector, the transfer rate decreases to reach a minimum value at the output of the module. This implies that stagnation conditions take place at this stage and that both fluid and PV cells achieve their maximum temperature.

3. Electrical models

To evaluate the electrical performances of the PV cell/module/array, various works have been conducted with the aim of developing physical models that imitate the electrical behavior of the PV cell. From an experimental point of view, a PV device is considered as a PN junction excited with light. Namely, the photovoltaic phenomenon converts coming light from the sun into electricity, which could be exploited in diverse domestic and industrial applications. According to the fluctuation of solar irradiance and temperature, the PV cell performance varies (Y. Chaibi et al., 2019b). Hence, the evaluation of these later required the use of equivalent-circuit models.

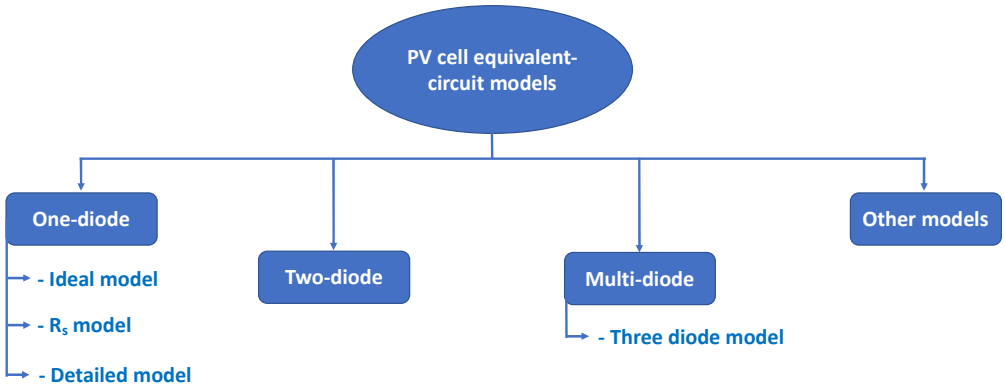

Fig. 8: Different equivalent-circuit models.

Historically, the evolution of theses equivalent-circuit configurations has developed from ideal to accurate models. Each model is characterized by its complexity of modeling, and the accuracy of imitating the real current-voltage (I-V) characteristics of the PV cell. In **Fig.8**, the most discussed models in the literature are presented, based on the number of used diodes, the classification is provided for each model. The one-diode model represents the basic

configuration and has been improved by adding resistances to the ideal representation. The double and the three diode models represent extensions of the single-diode configuration by adding other diodes in parallel.

3.1. One-diode model

a) Ideal model (3PM)

To perform the ideal behavior of the PV cell, the configuration in **Fig.9** displays the ideal equivalent-circuit model. This latter is represented by a source of current in parallel with a diode to design the PN junction operating without taking into consideration PV cell losses. From an experimental point of view, this model does not reflect the real electrical behavior of the PV cell, and this is via the provided current-voltage (I-V) characteristics.

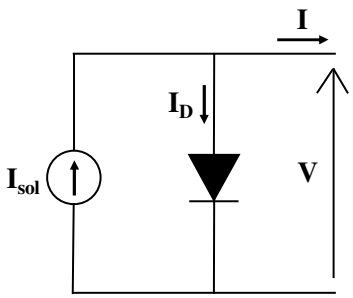

Fig. 9: Ideal model of the PV cell.

The output current I of this configuration is expressed by the following equation (Shockley, 1949):

$$I = I_{sol} - I_s\left\{exp\left[\frac{qV}{K\gamma TN_c} - 1\right]\right\} \quad (42)$$

where, I_{sol}, I_s are respectively the photo-generated and the saturation current, V is the output voltage. K and q represent the Boltzmann constant and the electron charge, respectively. γ is the ideality factor and N_c is the number of cells connected in series.

The main advantage of the ideal model is the simplicity of the current equation (See **Eq.(42)**), and this is because of the limited number of required parameters for PV cell modeling (Three parameters) (Mahmoud and El-Saadany, 2015). Historically, Rauschenbach initiated the ideal model and reclaimed that this configuration could only explain the basic theory of the PN junction (Rauschenbach, 1980). In the same context, Silvestre et al. proposed a modeling and simulation procedure of this model under PSpice environment. The

main objective of this proposition is to develop a sub-circuit of the ideal PV cell in order to perform graphically its corresponding I-V characteristics for different ranges of solar irradiance and temperature (Silvestre and Castan, 2013). Most of the discussed studies claim that the ideal model is not appropriate to imitate the real electrical behavior of the PV device (Rauschenbach, 1980; Sarkar, 2016). However, Some authors adopted improved versions to correct partially what was claimed. In (Mahmoud et al., 2012), Mahmoud et al. proposed improvements on the mathematical equations in order to avoid iterative calculation and simplify the design of the PV cell (Mahmoud et al., 2012). Also, a correction of the PV model behavior under low-irradiance is performed (Mahmoud and El-Saadany, 2015).

b) R_s model (4PM)

Based on reported works about PV cell modeling, the ideal model represents just a basic demonstration of the PV device theory and cannot be taken into account to analyze real PV cell performances. Thus, the modeling of losses and metal contacts at the level of the PN junction is expressed by adding resistance in series to the ideal model (Chenni et al., 2007; Walker, 2001). Namely, the simplified equivalent-circuit model (R_s model).

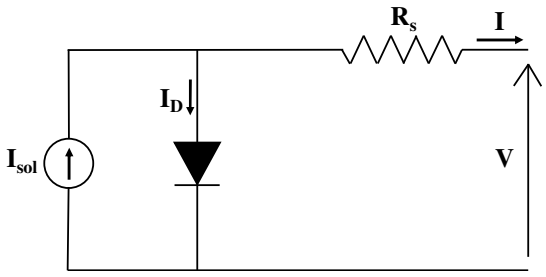

Fig. 10: Simplified equivalent circuit model of the PV cell.

The electrical representation of the R_s model is shown in **Fig.10**. The generated current by this configuration is expressed by **Eq.(43)** as follows:

$$I = I_{sol} - I_s \left\{ exp \left[\frac{q}{K\gamma T N_c} (V + IR_s) - 1 \right] \right\} \quad \textbf{(43)}$$

In the literature, the R_s model has been deployed by various authors (Chin et al., 2015; Khezzar et al., 2014; Walker, 2001). The first apparition reported by Rauschenbach et al. demonstrated theoretically the effect of the series resistance on the ideal theory of PV cell (Rauschenbach, 1980). Then, Walker et al. adopted this model due to the moderate complexity and the accurate results especially on the shape of the I-V curves (Walker, 2001). Chenni et al. reported that the simplified model exhibits more accurate I-V curves than a

model which neglects R_s, and insisted on the exact extraction of the R_s value due to its influence on the open-circuit voltage V_{oc} (Chenni et al., 2007). Most of the discussed works in the literature compared the R_s model I-V curves with manufacturer datasheets (Bellini et al., 2009; Celik and Acikgoz, 2007; Khezzar et al., 2014). As well in (Khezzar et al., 2014), authors compared improved modeling of the R_s model with other configurations such as detailed single-diode and double-diode models. The assessed results demonstrate that the proposed model provides accurate I-V characteristics for different module technologies (Khezzar et al., 2014).

c) R_{sh} model (5PM)

As the most adopted configuration in imitating the electrical behavior of the PV cell, the R_{sh} model provides an improvement of the R_s configuration by adding a parallel resistance called the shunt resistance (R_{sh}). This latter takes into consideration the current leaks that occur all over the PV a cell (Chaibi et al., 2018).

Fig.11 exhibits the scheme of the one-diode equivalent-circuit mode, the output current can be written as (Y. Chaibi et al., 2019c; De Soto et al., 2006; Villalva et al., 2009):

$$\boldsymbol{I = I_{sol} - I_s\left\{exp\left[\frac{q}{K\gamma TN_c}(V + IR_s) - 1\right]\right\} - \frac{V+R_sI}{R_{sh}}}$$

(44)

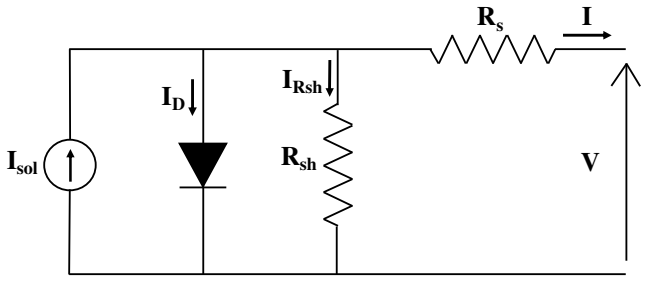

Fig. 11: Detailed single-diode model (R_{sh} model).

In the literature, this configuration has been adopted widely in different areas, its main advantage is the good balance between modeling complexity and accuracy (Chaibi et al., 2020). Accordingly, the authors proposed various techniques in order to evaluate the electrical performances of the R_{sh} model. Daniel et al. adopted the first analytical solution in order to analyze the one-diode model response under dark and illuminated conditions. The obtained

I-V curves were satisfactory with an estimated error of 10% (Chan and Phang, 1987, 1984). In the same context, Chegaar et al. proposed a comparative study of different analytical

methods to choose which technique is more accurate under illuminated conditions (Chegaar et al., 2004, 2003). In the last decades, many works have been conducted with the aim of improving the accuracy of the R_{sh} model. In (De Soto et al., 2006), De Soto et al. adopted a semi-empirical equation taking into account solar irradiance and temperature to provide accurate I-V characteristics. The obtained results are compared to a developed model by Sandia laboratory (Fanney et al., 2002); and experimental data for different module technologies (King et al., 2004, 1997). By improving the mathematical analysis of the R_{sh} model, Lo Brano et al. proposed an improved modeling procedure of the one-diode model by introducing a thermal factor to correct the I-V shape for temperature variations (Lo Brano et al., 2010). Villalva et al. proposed a novel iterative process to find the optimal modeling parameters (Villalva et al., 2009). Because the iterative process increases the computation time, many works adopted only provided data by the manufacturer to model the PV cell (Chaibi et al., 2018; Peng et al., 2014; Siddiqui and Abido, 2013). Recently, metaheuristics and machine learning-based techniques have been employed to model the PV device (Chin et al., 2015; Maria and Yassine, 2020; Pillai and Rajasekar, 2018). Most of the reported techniques in the literature proved high accuracy with low errors (Maria and Yassine, 2020; Pillai and Rajasekar, 2018).

3.2. Two-diode model (7PM)

According to the weather conditions, solar irradiance and temperature fluctuations affect the PV cell performances (Y. Chaibi et al., 2019a; Ishaque et al., 2011a). Hence, the PV device model has been improved to cover limitations at every climate fluctuation range. Many works reported that the R_{sh} model proved high accuracy especially at a high level of climate variation. However, its performances decrease at the low-fluctuations of irradiance and temperature (Ishaque et al., 2011a). To overcome this issue, the two-diode model (see **Fig.12**) is proposed, this configuration consists of two diodes in parallel which implies the use of double Shockley equations (Shockley, 1949).

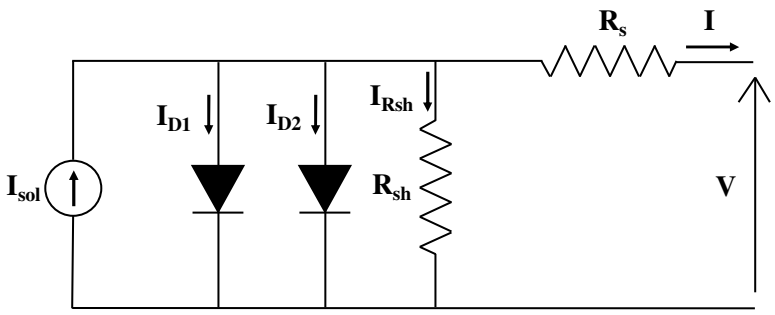

Fig. 12: Double-diode model of the PV cell.

The output current of the double-diode model is expressed by the following equation (Ishaque et al., 2011a; Kumar et al., 2019):

$$I = I_{sol} - I_{s1}\left\{exp\left[\frac{q}{K\gamma_1 TN_c}(V + IR_s) - 1\right]\right\} - I_{s2}\left\{exp\left[\frac{q}{K\gamma_2 TN_c}(V + IR_s) - 1\right]\right\} - \frac{V+R_sI}{R_{sh}} \quad \textbf{(45)}$$

Eq.(45) is characterized by the complexity of modeling because of the remarkable number of unknown parameters (seven parameters), which involves the use of approximations or numerical techniques. In the literature, researchers proposed many methods with the aim of describing the electrical properties of the PV cell. Stutenbaeumer et al. discussed the effect of the shunt and the series resistances on the I-V shape under dark conditions, the founded results demonstrate that the performances of the double-diode model are accurate for crystalline and amorphous technologies (Stutenbaeumer and Mesfin, 1999). Also, Daniel et al. developed a method based only on the provided electrical points by the manufacturer. In the last decades, numerical methods based on artificial intelligence have been investigated to resolve the problem of modeling complexity (Jordehi, 2016; Pillai and Rajasekar, 2018). Accordingly in (Sandrolini et al., 2010), Sandrolini et al. used particle swarm optimization (PSO) to obtain the physical parameters of the PV cell. Furthermore, Gao et al. adopted a novel LambertW based method to discuss fitness compared to other techniques (Gao et al., 2016). Most of the numerical methods produce an increase in computational time because of the important number of iterations. To reduce this latter, Ishaque et al. proposed an efficient technique with high accuracy and fast response (Ishaque et al., 2011a, 2011b).

3.3. Multi-diode model

Recently, with the evolution of numerical methods, the solution of any equation becomes easiest as it was in the past. This latter encourages the adjustment of previous configurations of the PV cell to multi-diode models (Pandey and Sandhu, 2015; Soon et al., 2014). Accordingly, the three-diodes model adopts the same configuration in **Fig.12** with three diodes. Also, the output current of this model can be expressed by the following equation:

$$I = I_{sol} - I_{s1}\left\{exp\left[\frac{q}{K\gamma_1 TN_c}(V + IR_s) - 1\right]\right\} \ldots - I_{sn}\left\{exp\left[\frac{q}{K\gamma_n TN_c}(V + IR_s) - 1\right]\right\} - \frac{V+R_sI}{R_{sh}} \quad \textbf{(46)}$$

where, *n* represents the number of the used Shockley diodes which is 3.

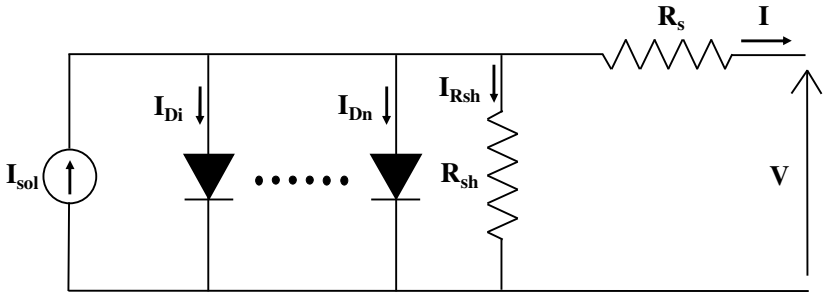

Fig. 13: Multi diodes model of the PV cell.

This configuration in **Fig.13** has been employed by a limited number of authors because of its modeling complexity. Accordingly, metaheuristics methods have been used to resolve this problem (Allam et al., 2016; Qais et al., 2019). Thus, In (Khanna et al., 2015), Vandana et al. proposed modeling of the three-diodes model which can provide better I-V accuracy than single and double diode models (Khanna et al., 2015). Also, Allam et al. adopted a moth-flame optimization algorithm to model the three-diodes configuration, the obtained results shown high performances compared to literature (Allam et al., 2016).

3.4. Other models

Above all reported equivalent-circuit models, other configurations have been proposed. Kurobe et al. proposed a novel model with two diodes instead of one including diffusion and recombination's current of the PV cell (Kurobe and Matsunami, 2005). As well, Mazahri et al. and de castro et al. initiated an improved configuration to model organic cells (De Castro et al., 2016; Mazhari, 2006). But, most of these models are avoided due to their limited performances.

3.5. Experimental validation

In this section, a parametric study is performed to exhibit the electrical performances of different equivalent-circuit models. Indeed, Siemens SP75 PV panel is adopted to proceed with detailed modeling using some of the most used configurations discussed in the previous section. Thus, the modeling task is carried out to extract the unknown parameters of each model using developed and accurate techniques from the literature (see **Table 2**). Namely, Chaibi et al. algorithms are adopted to model the 3PM and 5PM (Chaibi et al., 2020; Y. Chaibi et al., 2019a), Khezzar et al. for the 4PM (Khezzar et al., 2014), Villalva et al. for the 5PM (Villalva et al., 2009); and Ishaque et al. for the 7PM (Ishaque et al., 2011a).

Table 2: Adopted modeling techniques for each equivalent-circuit model.

Equivalent-circuit model	Modeling technique
Ideal model (3PM)	Chaibi et al. (Y. Chaibi et al., 2019a)
R_s model (4PM)	Khezzar et al. (Khezzar et al., 2014)
R_{sh} model (5PM)	Chaibi et al. (Chaibi et al., 2018), Villalva et al. (Villalva et al., 2009)
Double-diode model (7PM)	Ishaque et al. (Ishaque et al., 2011a)

a) Chaibi et al. (Chaibi et al., 2020; Y. Chaibi et al., 2019a):

This method involves using the information provided by the manufacturer to determine the unknown parameters of each model. In fact, the adopted process to extract the R_{sh} model parameters is based on iterating the shunt resistance and compute other parameters using a set of manufacturer based-equations (Chaibi et al., 2020). Further, to find the unknown parameters of the ideal model, a modification is done on the Chaibi et al. method (Chaibi et al., 2018). Accordingly, the ideal model requires only three parameters to compute the corresponding I-V characteristics. These parameters *are* I_{ph}, γ and I_s. For this reason, we have assumed that shunt resistance is infinite and the series one is zero (Chaibi et al., 2018).

b) Khezzar et al. (Khezzar et al., 2014):

The Khezzar et al. techniques adopted corrections on the R_s model equations to enhance the 4PM performances. Indeed, a modification on both equations of open-circuit voltage and maximum power point voltage is elaborated in order to take into consideration the solar irradiance and temperature fluctuations (Khezzar et al., 2014).

c) Villalva et al. (Villalva et al., 2009):

Villalva's et al. technique represents one of the most used methods to design the R_{sh} model in the literature. Villalva's algorithm includes an iterative process of the diode ideality factor and a numerical calculation of other parameters by using mathematical expressions. The convergence condition of this iterative process is to match the computed power at MPP with the experimental one taken from the manufacturer datasheet at Standard test conditions (STC) ($G=1000W/m^2$, $T_c = 25°C$, A.M = 1.5) (Villalva et al., 2009).

d) Ishaque et al. (Ishaque et al., 2011a)

By reason of its modeling complexity, the double-diode model is known by an important number of unknowns, which are seven parameters to find. Thus, Ishaque et al technique represented a solution to compute these parameters (Ishaque et al., 2011a). In fact, some

approximations are adopted to reduce the number of unknowns. Accordingly, the authors assumed that both saturation currents are equal. In addition, the diode ideality factors are replaced by constants. Then, other parameters are computed by iterating both series and shunt resistances until achieving a good agreement between experimental and calculated power (Ishaque et al., 2011a).

By applying the reported techniques in **Table 2** on the Siemens SP75 PV module. The founded parameters are summarized in **Table 3**, and then used to plot corresponding I-V characteristics for each model.

Table 3: Extracted parameters at STC of the SP75 PV module using literature based techniques.

Modeling method	**Extracted parameters**				
	I_{sol} [A]	**γ**	**I_S [A]**	**R_s [Ω]**	**R_{sh} [Ω]**
Chaibi et al. (Y. Chaibi et al., 2019a)	4.8	2.4188	$2.94*10^{-4}$	-	-
Khezzar et al. (Khezzar et al., 2014)	4.8	1.5619	$1.43*10^{-6}$	0.25	-
Chaibi et al. (Chaibi et al., 2018)	4.8	1.5352	$1.10*10^{-6}$	0.26	2670
Villalva et al. (Villalva et al., 2009)	4.8	1.3	$6.95*10^{-8}$	0.33	236
Ishaque et al. (Ishaque et al., 2011a)	4.8	γ_1=1 γ_2=1.2	$I_{S1}= I_{S2}= 3.09*10^{-10}$	0.45	129

Fig.14 provides generated I-V curves at STC using each model separately. These I-V characteristics are plotted together with the experimental curve to demonstrate the fitting level of each model comparing to the experimental reference. It is worth mentioning that the experimental data are extracted carefully using the reported methodology by Chaibi et al. (Yassine Chaibi et al., 2019). To assess this difference between the discussed models and the experimental curve, three zones are mentioned and zoomed at the level of the I-V curves (see **Fig.14**). From zone 1, it is clear that both 5PM and 4PM agree well with the experimental curve. However, other models such as 7PM and 3PM are far away from the experimental data. In zone 2, the 5PM and 4PM maintain the good agreement by fitting accurately the experimental data. From zone 3, it is remarked that all models are very close to the experimental data with the superiority of the 5PM.

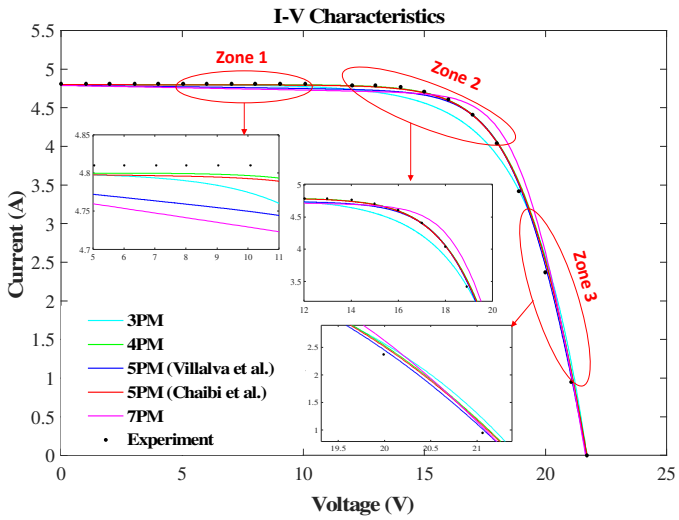

Fig. 14: Experimental and generated I-V characteristics at STC using different methods from the literature.

From **Fig.14**, Some conclusions related to the use of equivalent-circuit configurations in PV modeling are presented as follows:

- The 3PM represents only an ideal shape of the I-V characteristic and cannot be adopted to perform the real behavior of the PV cell.
- The 4PM exhibits high performances which are very close to those provided by the 5PM, and this explains why most of the authors neglect the shunt resistance.
- The 5PM is the most suitable to forecast the electrical performances of PV modules. Besides, it is observed that the modeling technique could affect the performance of this model, and this is clear by the remarked disagreement between corresponding I-V curves to Chaibi et al. and Villalva et al. method.
- The 7PM requires complex modeling techniques, and its performances are modest. Consequently, the good compromise between complexity and accuracy supports the option of using the 5PM instead of the 7PM.

To assess the electrical behavior of each reported equivalent-circuit in **Table 2**, the PV module efficiency of the SP75 PV panel is computed for a large variation of cell temperature and solar irradiance. Then, the results are plotted in **Fig.15** for each equivalent-circuit model. Form this figure, it is clear that for low-irradiances (300 W/m^2<), 5PM and 4PM provide good results compared to other models. Further, Chaibi et al. technique outweighs the Villalva et al. method, which explains the influence of modeling technique on PV performances. Besides, for irradiances above 300 W/m^2, the double-diode model presents accurate results, which explains the good response of the 7PM for high fluctuations of irradiance.

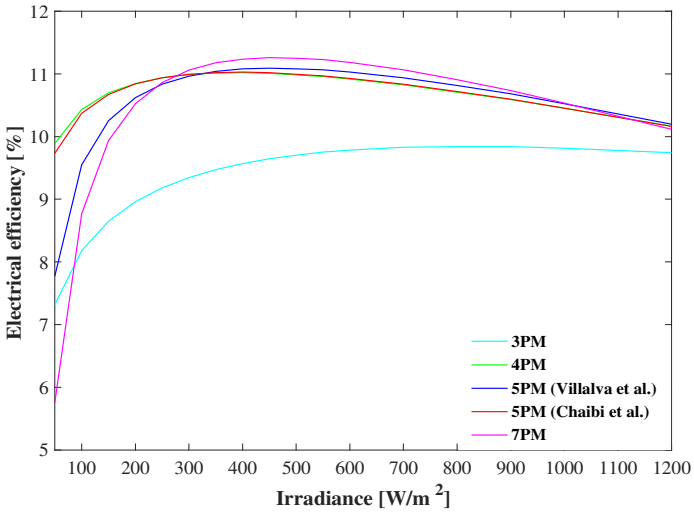

Fig. 15: Electrical efficiencies of reported equivalent-circuit models for a large variation of irradiance.

4. Some limitations of the electrical models

A hybrid solar panel uses the heat released by the photovoltaic cells to heat a heat transfer fluid (liquid or air), which improves the efficiency of the PV cells while recovering useful solar heat (Tina et al., 2010; Zondag, 2008). Several electrical models have been developed to analyze only the electrical performance of the PV panels. Most of these models adopted the single-diode approach to perform the I-V characteristics (Bechouat et al., 2019; Catelani et al., 2016; Schön, 2017; Slimani et al., 2017; Tina et al., 2010). However, in some applications, the double-diode model is preferred due to its good performance (Babu and Ponnambalam, 2018; Pillai and Rajasekar, 2018; Waliullah et al., 2015). In this section, some limitations of the electrical models to imitate an accurate electrical behavior of PV/T systems are reported according to different works from the literature. For this, Giuseppe et al. proposed a numerical study to investigate the effect of the temperature gradient on the PV module/array and to analyze the influence of temperature on the I-V curves for different schemes of cell connection (Tina et al., 2010). In the same context, Lambarski et al. (Lambarski, 1984) reported that the influence of temperature gradient difference on cells connected in series is negligible. However, in parallel connection, the efficiency of the PV cell is significantly affected (until 17% of losses). The reason for these losses is that the temperature of the PV/T module is not uniform, which causes a problem in tracking the global MPP (Zondag, 2008). Bechouat et al. (Bechouat et al., 2019) reported that the increase of temperature at the junction levels PV cells affects negatively the electrical characteristics of PV modules and limits their electrical performances. As a solution, the authors proposed a

numerical PV/T model based on both 2D lookup table together with the single-diode equivalent-circuit model to simulate the effect of temperature on the overall performances of the system. This approach provided accurate results compared to the experiments (Bechouat et al., 2019). Further, Catelani et al. (Catelani et al., 2016) adopted the single and double-diode circuits to describe the electrical performances of a PV/T concentrator. This model takes into consideration the effect of the concentration factor and the environmental conditions. Slimani et al. (Slimani et al., 2017) proposed a thermo-electrical model based on the single-diode circuit to evaluate the performances of various PV/T collectors and provide the temperature evolution at each level of the PV module.

As indicated in previous works, the effect of temperature on the performance of the system is not yet simulated correctly with existing electrical models. It is necessary to develop other approaches (combining thermal and electrical aspects) to consider the effect of temperature on the overall performance of the system, taking into account geometrical and climatic aspects.

5. Conclusion

In this paper, two thermal models (QSTM and TTM) and various electrical models have been developed to study the energy performance of the PV/T system. The main obtained results from the present investigation can be summarized as the following:

- Both physical models (QSTM and TTM) produce similar results.
- The computing time can be reduced by using QST model.
- The single-diode and the double-diode models are the most suitable to design the PV/T electrical performances.
- Temperature has a significant effect on the electrical performance of the system. Electrical models need to be refined and improved to account this effect in the design of these technologies.

Acknowledgments

The authors sincerely acknowledge the fund received from EUROSTAR programme under the project PV-SolAir (E!113591).

References

Abdul Hamid, S., Yusof Othman, M., Sopian, K., Zaidi, S.H., 2014. An overview of photovoltaic thermal combination (PV/T combi) technology. Renew. Sustain. Energy Rev. 38, 212–222. https://doi.org/10.1016/j.rser.2014.05.083

Agrawal, S., Tiwari, G.N., 2013. Overall energy, exergy and carbon credit analysis by different type of hybrid photovoltaic thermal air collectors. Energy Convers. Manag. 65, 628–636. https://doi.org/10.1016/j.enconman.2012.09.020

Allam, D., Yousri, D.A., Eteiba, M.B., 2016. Parameters extraction of the three diode model for the multi-crystalline solar cell/module using Moth-Flame Optimization Algorithm. Energy Convers. Manag. 123, 535–548. https://doi.org/10.1016/j.enconman.2016.06.052

Babu, C., Ponnambalam, P., 2018. The theoretical performance evaluation of hybrid PV-TEG system. Energy Convers. Manag. 173, 450–460. https://doi.org/10.1016/j.enconman.2018.07.104

Bambrook, S.M., Sproul, A.B., 2016. A solvable thermal circuit for modelling PVT air collectors. Sol. Energy 138, 77–87. https://doi.org/10.1016/j.solener.2016.09.007

Barone, G., Buonomano, A., Forzano, C., Palombo, A., Panagopoulos, O., 2019. Experimentation, modelling and applications of a novel low-cost air-based photovoltaic thermal collector prototype. Energy Convers. Manag. 195, 1079–1097. https://doi.org/10.1016/j.enconman.2019.04.082

Bechouat, M., Sedraoui, M., Feraga, C.E., Aidoud, M., Kahla, S., 2019. Modeling and Fuzzy MPPT Controller Design for Photovoltaic Module Equipped with a Closed-Loop Cooling System. J. Electron. Mater. 48, 5471–5480. https://doi.org/10.1007/s11664-019-07243-1

Bellini, A., Bifaretti, S., Iacovone, V., Cornaro, C., 2009. Simplified model of a photovoltaic module. 2009 Appl. Electron. Int. Conf. AE 2009 47–52.

Brinkworth, B.J., 2002. Coupling of Convective and Radiative Heat Transfer in PV Cooling Ducts. J. Sol. Energy Eng 124, 250–255.

Catelani, M., Ciani, L., Kazimierczuk, M.K., Reatti, A., 2016. Matlab PV solar concentrator performance prediction based on triple junction solar cell model. Meas. J. Int. Meas. Confed. 88, 310–317. https://doi.org/10.1016/j.measurement.2016.03.046

Celik, A.N., Acikgoz, N., 2007. Modelling and experimental verification of the operating current of mono-crystalline photovoltaic modules using four- and five-parameter models. Appl. Energy 84, 1–15. https://doi.org/10.1016/j.apenergy.2006.04.007

Chaibi, Y., Allouhi, A., Malvoni, M., Salhi, M., Saadani, R., 2019a. Solar irradiance and temperature influence on the photovoltaic cell equivalent-circuit models. Sol. Energy 188, 1102–1110. https://doi.org/10.1016/j.solener.2019.07.005

Chaibi, Y., Allouhi, A., Salhi, M., 2020. A simple iterative method to determine the electrical parameters of photovoltaic cell. J. Clean. Prod. 122363. https://doi.org/10.1016/j.jclepro.2020.122363

Chaibi, Y., Allouhi, A., Salhi, M., El-jouni, A., 2019b. Annual performance analysis of

different maximum power point tracking techniques used in photovoltaic systems. Prot. Control Mod. Power Syst. 4. https://doi.org/10.1186/s41601-019-0129-1

Chaibi, Y., ElRhafiki, T., Simón-Allué, R., Guedea, I., Luaces, S.C., Gajate, O.C., Kousksou, T., Zeraouli, Y., 2021a. Air-based hybrid Photovoltaic/Thermal systems: A review Y. J. Clean. Prod. https://doi.org/10.1016/j.jclepro.2021.126211

Chaibi, Yassine, Malvoni, M., Allouhi, A., Mohamed, S., 2019. Data on the I-V characteristics related to the SM55 monocrystalline PV module at various solar irradiance and temperatures. Data Br. 104527. https://doi.org/10.1016/j.dib.2019.104527

Chaibi, Y., Malvoni, M., El Rhafiki, T., Kousksou, T., Zeraouli, Y., 2021b. Artificial neural-network based model to forecast the electrical and thermal efficiencies of PVT air collector systems. Clean. Eng. Technol. 4, 100132. https://doi.org/10.1016/j.clet.2021.100132

Chaibi, Y., Salhi, M., El-Jouni, A., 2019c. Sliding mode controllers for standalone PV systems: Modeling and approach of control. Int. J. Photoenergy 2019, 1–12. https://doi.org/10.1155/2019/5092078

Chaibi, Y., Salhi, M., El-jouni, A., Essadki, A., 2018. A new method to extract the equivalent circuit parameters of a photovoltaic panel. Sol. Energy 163, 376–386. https://doi.org/10.1016/j.solener.2018.02.017

Chan, D.S.H., Phang, J.C.H., 1987. Analytical Methods for the Extraction of Solar-Cell Single-and Double-Diode Model Parameters from I-V Characteristics. IEEE Trans. Electron Devices 34, 286–293. https://doi.org/10.1109/T-ED.1987.22920

Chan, D.S.H., Phang, J.C.H., 1984. A Method for the Direct Measurement of Solar Cell Shunt Resistanc 23, 381–383.

Chegaar, M., Ouennoughi, Z., Guechi, F., 2004. Extracting dc parameters of solar cells under illumination. Vacuum 75, 367–372. https://doi.org/10.1016/j.vacuum.2004.05.001

Chegaar, M., Ouennoughi, Z., Guechi, F., Langueur, H., 2003. Determination of solar cells parameters under illuminated conditions. J. Electron Devices 2, 17–21.

Chenni, R., Makhlouf, M., Kerbache, T., Bouzid, A., 2007. A detailed modeling method for photovoltaic cells. Energy 32, 1724–1730. https://doi.org/10.1016/j.energy.2006.12.006

Chin, V.J., Salam, Z., Ishaque, K., 2015. Cell modelling and model parameters estimation techniques for photovoltaic simulator application: A review. Appl. Energy 154, 500–519. https://doi.org/10.1016/j.apenergy.2015.05.035

Chow, T.T., 2003. Performance analysis of photovoltaic-thermal collector by explicit dynamic model. Sol. Energy 75, 143–152. https://doi.org/10.1016/j.solener.2003.07.001

De Castro, F., Laudani, A., Riganti Fulginei, F., Salvini, A., 2016. An in-depth analysis of the modelling of organic solar cells using multiple-diode circuits. Sol. Energy 135, 590–597. https://doi.org/10.1016/j.solener.2016.06.033

De Soto, W., Klein, S.A., Beckman, W.A., 2006. Improvement and validation of a model for photovoltaic array performance. Sol. Energy 80, 78–88. https://doi.org/10.1016/j.solener.2005.06.010

Diwania, S., Agrawal, S., Siddiqui, A.S., Singh, S., 2020. Photovoltaic–thermal (PV/T) technology: a comprehensive review on applications and its advancement. Int. J. Energy Environ. Eng. 11, 33–54. https://doi.org/10.1007/s40095-019-00327-y

Elsafi, A., Gandhidasan, P., 2015. Performance of a Photovoltaic or Thermal Double-Pass Solar Air Heater with Different Fin Configurations. J. Clean Energy Technol. 3, 28–33. https://doi.org/10.7763/jocet.2015.v3.163

European Commission, 2020. Commission Implmenting Regulation (EU) 2020/2156 of 14 October 2020 detailing the technical modalities for the effective implementation of an optional common Union scheme for rating the smart readiness of buildings. Off. J. Eur. Union 2156, 25–29.

Evans, D.L., 1981. Simplified method for predicting photovoltaic array output. Sol. energy 27, 555–560.

Fanney, A.H., Dougherty, B.P., Davis, M.W., 2002. EVALUATING BUILDING INTEGRATED PHOTOVOLTAIC PERFORMANCE MODELS By Building and Fire Research Laboratory National Institute of Standards and Technology Reprinted from the Proceedings of the New Orleans , Louisiana NOTE : This paper is a contribution of the. Technology.

Gao, X., Cui, Y., Hu, J., Xu, G., Yu, Y., 2016. Lambert W-function based exact representation for double diode model of solar cells: Comparison on fitness and parameter extraction. Energy Convers. Manag. 127, 443–460. https://doi.org/10.1016/j.enconman.2016.09.005

Good, C., 2016. Environmental impact assessments of hybrid photovoltaic–thermal (PV/T) systems–A review. Renew. Sustain. Energy Rev. 55, 234–239.

Hazami, M., Riahi, A., Mehdaoui, F., Nouicer, O., Farhat, A., 2016. Energetic and exergetic performances analysis of a PV/T (photovoltaic thermal) solar system tested and simulated under to Tunisian (North Africa) climatic conditions. Energy 107, 78–94.

Hosseinzadeh, M., Salari, A., Sardarabadi, M., Passandideh-Fard, M., 2018. Optimization and parametric analysis of a nanofluid based photovoltaic thermal system: 3D numerical model with experimental validation. Energy Convers. Manag. 160, 93–108.

Hussain, F., Othman, M.Y.H., Sopian, K., Yatim, B., Ruslan, H., Othman, H., 2013. Design development and performance evaluation of photovoltaic/thermal (PV/T) air base solar collector. Renew. Sustain. Energy Rev. 25, 431–441. https://doi.org/10.1016/j.rser.2013.04.014

Ibrahim, A., Othman, M.Y., Ruslan, M.H., Mat, S., Sopian, K., 2011. Recent advances in flat plate photovoltaic/thermal (PV/T) solar collectors. Renew. Sustain. energy Rev. 15, 352–365. https://doi.org/10.1016/j.rser.2010.09.024

Ishaque, K., Salam, Z., Taheri, H., 2011a. Simple, fast and accurate two-diode model for photovoltaic modules. Sol. Energy Mater. Sol. Cells 95, 586–594. https://doi.org/10.1016/j.solmat.2010.09.023

Ishaque, K., Salam, Z., Taheri, H., Syafaruddin, 2011b. Modeling and simulation of photovoltaic (PV) system during partial shading based on a two-diode model. Simul. Model. Pract. Theory 19, 1613–1626. https://doi.org/10.1016/j.simpat.2011.04.005

Jia, Y., Alva, G., Fang, G., 2019. Development and applications of photovoltaic–thermal systems: A review. Renew. Sustain. Energy Rev. 102, 249–265. https://doi.org/10.1016/j.rser.2018.12.030

Jordehi, A.R., 2016. Parameter estimation of solar photovoltaic (PV) cells: A review. Renew. Sustain. Energy Rev. 61, 354–371. https://doi.org/10.1016/j.rser.2016.03.049

Joshi, A.S., Tiwari, A., 2007. Energy and exergy efficiencies of a hybrid photovoltaic-thermal (PV/T) air collector. Renew. Energy 32, 2223–2241. https://doi.org/10.1016/j.renene.2006.11.013

Joshi, A.S., Tiwari, A., Tiwari, G.N., Dincer, I., Reddy, B. V, 2009. Performance evaluation of a hybrid photovoltaic thermal (PV/T)(glass-to-glass) system. Int. J. Therm. Sci. 48, 154–164.

Khanna, V., Das, B.K., Bisht, D., Vandana, Singh, P.K., 2015. A three diode model for industrial solar cells and estimation of solar cell parameters using PSO algorithm. Renew. Energy 78, 105–113. https://doi.org/10.1016/j.renene.2014.12.072

Khezzar, R., Zereg, M., Khezzar, A., 2014. Modeling improvement of the four parameter model for photovoltaic modules. Sol. Energy 110, 452–462. https://doi.org/10.1016/j.solener.2014.09.039

King, D.L., Kratochvil, J. a, Boyson, W.E., 2004. Photovoltaic array performance model. Online 8, 1–19. https://doi.org/10.2172/919131

King, D.L., Kratochvil, J.A., Boyson, W.E., 1997. Field experience with a new performance characterization procedure for photovoltaic arrays. United States.

Kousksou, T., Allouhi, A., Belattar, M., Jamil, A., El Rhafiki, T., Arid, A., Zeraouli, Y., 2015. Renewable energy potential and national policy directions for sustainable development in Morocco. Renew. Sustain. Energy Rev. 47, 46–57. https://doi.org/10.1016/j.rser.2015.02.056

Kumar, A., Baredar, P., Qureshi, U., 2015. Historical and recent development of photovoltaic thermal (PVT) technologies. Renew. Sustain. Energy Rev. 42, 1428–1436. https://doi.org/10.1016/j.rser.2014.11.044

Kumar, S., Sahu, H.S., Nayak, S.K., 2019. Estimation of MPP of a Double Diode Model PV Module from Explicit I-V Characteristic. IEEE Trans. Ind. Electron. 66, 7032–7042. https://doi.org/10.1109/TIE.2018.2877116

Kurobe, K.I., Matsunami, H., 2005. New two-diode model for detailed analysis of multicrystalline silicon solar cells. Japanese J. Appl. Physics, Part 1 Regul. Pap. Short Notes Rev. Pap. 44, 8314–8321. https://doi.org/10.1143/JJAP.44.8314

Lambarski, T.J., 1984. Electrical design guidelines for photovoltaic/thermal systems. United States.

Lamnatou, C., Chemisana, D., 2017. Photovoltaic/thermal (PVT) systems: A review with emphasis on environmental issues. Renew. Energy 105, 270–287. https://doi.org/10.1016/j.renene.2016.12.009

Lo Brano, V., Orioli, A., Ciulla, G., Di Gangi, A., 2010. An improved five-parameter model for photovoltaic modules. Sol. Energy Mater. Sol. Cells 94, 1358–1370. https://doi.org/10.1016/j.solmat.2010.04.003

Mahmoud, Y., El-Saadany, E., 2015. Accuracy improvement of the ideal PV Model. IEEE Trans. Sustain. Energy 6, 909–911. https://doi.org/10.1109/TSTE.2015.2412694

Mahmoud, Y., Xiao, W., Zeineldin, H.H., 2012. A simple approach to modeling and simulation of photovoltaic modules. IEEE Trans. Sustain. Energy 3, 185–186. https://doi.org/10.1109/TSTE.2011.2170776

Maria, M., Yassine, C., 2020. Machine learning based approaches for modeling the output power of photovoltaic array in real outdoor conditions. Electron. 9, 315.

https://doi.org/10.3390/electronics9020315

Mazhari, B., 2006. An improved solar cell circuit model for organic solar cells. Sol. Energy Mater. Sol. Cells 90, 1021–1033. https://doi.org/10.1016/j.solmat.2005.05.017

Pandey, P.K., Sandhu, K.S., 2015. Multi diode modelling of PV cell. India Int. Conf. Power Electron. IICPE 2015-May, 1–4. https://doi.org/10.1109/IICPE.2014.7115793

Patankar, S., 1980. Numerical heat transfer and fluid flow. Taylor & Francis.

Peng, L., Sun, Y., Meng, Z., 2014. An improved model and parameters extraction for photovoltaic cells using only three state points at standard test condition. J. Power Sources 248, 621–631. https://doi.org/10.1016/j.jpowsour.2013.07.058

Pillai, D.S., Rajasekar, N., 2018. Metaheuristic algorithms for PV parameter identification: A comprehensive review with an application to threshold setting for fault detection in PV systems. Renew. Sustain. Energy Rev. 82, 3503–3525. https://doi.org/10.1016/j.rser.2017.10.107

Qais, M.H., Hasanien, H.M., Alghuwainem, S., Nouh, A.S., 2019. Coyote optimization algorithm for parameters extraction of three-diode photovoltaic models of photovoltaic modules. Energy 187, 116001. https://doi.org/10.1016/j.energy.2019.116001

Rauschenbach, H. s. ., 1980. Solar Cell Array Design Handbook, Solar Cell Array Design Handbook. https://doi.org/10.1007/978-94-011-7915-7

Sandrolini, L., Artioli, M., Reggiani, U., 2010. Numerical method for the extraction of photovoltaic module double-diode model parameters through cluster analysis. Appl. Energy 87, 442–451. https://doi.org/10.1016/j.apenergy.2009.07.022

Sarhaddi, F., Farahat, S., Ajam, H., Behzadmehr, A., 2010a. Exergetic performance assessment of a solar photovoltaic thermal (PV/T) air collector. Energy Build. 42, 2184–2199. https://doi.org/10.1016/j.enbuild.2010.07.011

Sarhaddi, F., Farahat, S., Ajam, H., Behzadmehr, A., Mahdavi Adeli, M., 2010b. An improved thermal and electrical model for a solar photovoltaic thermal (PV/T) air collector. Appl. Energy 87, 2328–2339. https://doi.org/10.1016/j.apenergy.2010.01.001

Sarkar, M.N.I., 2016. Effect of various model parameters on solar photovoltaic cell simulation: a SPICE analysis. Renewables Wind. Water, Sol. 3. https://doi.org/10.1186/s40807-016-0035-3

Schön, G., 2017. Numerical Modelling of a Novel Pvt Collector At Cell Resolution.

Sellami, R., Amirat, M., Mahrane, A., Slimani, M.E.A., Arbane, A., Chekrouni, R., 2019. Experimental and numerical study of a PV/Thermal collector equipped with a PV-assisted air circulation system: Configuration suitable for building integration. Energy Build. 190, 216–234. https://doi.org/10.1016/j.enbuild.2019.03.007

Senthil Kumar, R., Puja Priyadharshini, N., Natarajan, E., 2016. Numerical and Experimental Investigation of Transient Thermal Behaviour on Solar Photovoltaic Thermal (Pv / T) Hybrid System.

Shahsavar, A., Ameri, M., 2010. Experimental investigation and modeling of a direct-coupled PV/T air collector. Sol. Energy 84, 1938–1958. https://doi.org/10.1016/j.solener.2010.07.010

Shockley, W., 1949. The Theory of p-n Junctions in Semiconductors and p-n Junction Transistors. Bell Syst. Tech. J. 28, 435--489.

Siddiqui, M.U., Abido, M., 2013. Parameter estimation for five- and seven-parameter photovoltaic electrical models using evolutionary algorithms. Appl. Soft Comput. J. 13, 4608–4621. https://doi.org/10.1016/j.asoc.2013.07.005

Silvestre, S., Castan, L., 2013. Modelling Photovoltaic Systems using PSpice, Journal of Chemical Information and Modeling. https://doi.org/10.1017/CBO9781107415324.004

Slimani, M.E.A., Amirat, M., Kurucz, I., Bahria, S., Hamidat, A., Chaouch, W.B., 2017. A detailed thermal-electrical model of three photovoltaic/thermal (PV/T) hybrid air collectors and photovoltaic (PV) module: Comparative study under Algiers climatic conditions. Energy Convers. Manag. 133, 458–476. https://doi.org/10.1016/j.enconman.2016.10.066

Soon, J.J., Low, K.S., Goh, S.T., 2014. Multi-dimension diode photovoltaic (PV) model for different PV cell technologies. IEEE Int. Symp. Ind. Electron. 2496–2501. https://doi.org/10.1109/ISIE.2014.6865012

Stutenbaeumer, U., Mesfin, B., 1999. Equivalent model of monocrystalline, polycrystalline and amorphous silicon solar cells. Renew. Energy 18, 501–512. https://doi.org/10.1016/S0960-1481(98)00813-1

Su, D., Jia, Y., Huang, X., Alva, G., Tang, Y., Fang, G., 2016. Dynamic performance analysis of photovoltaic-thermal solar collector with dual channels for different fluids. Energy Convers. Manag. 120, 13–24. https://doi.org/10.1016/j.enconman.2016.04.095

Swinbank, W.C., 1963. Long-wave radiation from clear skies. Q. J. R. Meteorol. Soc. 89, 339–348.

Task 49 IEA, 2020. Solar Heat Integrations in Industrial Processes.

Task 60 IEA, 2020. Existing PVT systems and solutions 125. https://doi.org/10.18777/ieashc-task60-2020-0001

The european parliament, ., 2018. DIRECTIVE (EU) 2018/844 OF THE EUROPEAN PARLIAMENT AND OF THE COUNCIL of 30 May 2018 amending Directive 2010/31/EU on the energy performance of buildings. Off. J. Eur. Union EN L. https://doi.org/10.1007/3-540-47891-4_10

Tina, G., Cosentino, F., Notton, G., 2010. Effect of thermal gradient of electrical efficiency of hybrid PV/T. 25th Eur. Photovolt. Sol. energy Conf. Exhib. world Conf. Photovolt. energy Convers.

Tonui, J.K., Tripanagnostopoulos, Y., 2007. Improved PV/T solar collectors with heat extraction by forced or natural air circulation. Renew. Energy 32, 623–637. https://doi.org/10.1016/j.renene.2006.03.006

Vaishak, S., Bhale, P. V., 2019. Photovoltaic/thermal-solar assisted heat pump system: Current status and future prospects. Sol. Energy 189, 268–284. https://doi.org/10.1016/j.solener.2019.07.051

Villalva, M.G., Gazoli, J.R., Filho, E.R., 2009. Comprehensive Approach to Modeling and Simulation of Photovoltaic Arrays. IEEE Trans. Power Electron. 24, 1198–1208. https://doi.org/10.1109/TPEL.2009.2013862

Waliullah, M., Hossain, M.Z., Saha, S., 2015. On the implementation of two-diode model for photovoltaic-thermal systems. Procedia Eng. 105, 725–732. https://doi.org/10.1016/j.proeng.2015.05.063

Walker, G., 2001. Evaluating MPPT converter topologies using a matlab PV model. J. Electr.

Electron. Eng. Aust. 21, 49–55.

Yang, T., Athienitis, A.K., 2014. A study of design options for a building integrated photovoltaic/thermal (BIPV/T) system with glazed air collector and multiple inlets. Sol. Energy 104, 82–92. https://doi.org/10.1016/j.solener.2014.01.049

Yazdanifard, F., Ameri, M., 2018. Exergetic advancement of photovoltaic/thermal systems (PV/T): A review. Renew. Sustain. Energy Rev. 97, 529–553. https://doi.org/10.1016/j.rser.2018.08.053

Yu, Y., Yang, H., Peng, J., Long, E., 2019. Performance comparisons of two flat-plate photovoltaic thermal collectors with different channel configurations. Energy 175, 300–308. https://doi.org/10.1016/j.energy.2019.03.054

Zondag, H.A., 2008. Flat-plate PV-Thermal collectors and systems: A review. Renew. Sustain. Energy Rev. 12, 891–959. https://doi.org/10.1016/j.rser.2005.12.012